Ion Beam Analysis of
Lower Dimensional Structures

L.C. Feldman*

Department of Physics and Astronomy
Vanderbilt University
Nashville, TN 37215, USA

Abstract

The use of ion beam analysis for the characterization of lower dimensional structures is reviewed. Fundamental limitations as well as practical sources of uncertainty are described. A number of recent examples illustrate the useful information extracted by such analysis, and the critical role that ion beam analysis plays in modern materials science.

Contents

* E-mail: leonard.c.feldman@vanderbilt.edu

1. Introduction

A major theme within condensed matter physics and materials science is the creation and characterization of nanostructures, solids with characteristic dimensions less than 100 nm.

Ion beam technology is having a major influence on nanoscience, primarily through ion implantation of nanostructured solids, ion beam lithography at the nanoscale, finely focused ion beam technology, single ion implantation schemes and ion beam analysis. This paper considers some of the ways in which ion beams are impacting nanoscience characterization and analysis, with a special emphasis on the characterization of lower dimensional nanostructures. This paper describes the current limits of ion beam analysis and outstanding problems in the field. The emphasis in this paper will be on the use of ion scattering in the control of semiconductor surfaces, both for two dimensional problems (planar technologies) and zero dimensional problems (quantum dots). Ion beam analysis of thin films is a major field unto itself and has been applied to a large variety of thin film structures. In this paper we focus on the semiconductor dielectric interface, which is of extensive interest and illustrates many of the features and limitations of ion beam analysis.

I first review the basic concepts on ion beam analysis with an emphasis on the simple aspects of Rutherford backscattering (RBS). RBS in all its forms provides a vehicle for understanding the limitations and issues associated with the ion beam analysis. I then provide a detailed discussion of the limits of ion scattering in its various applications. Finally the applicability of these concepts to a number of nanoscience investigations is illustrated. The discussion will focus on the region of incident energies from 100 KeV to $\sim$2 MeV, the most used region for precision material analysis.

This paper is not meant to be a comprehensive or complete overview of ion scattering analysis. Rather it cites few examples, many from the author's work, that allow us to illustrate and discuss the advantages and limitations of ion scattering analysis at the nanoscale.
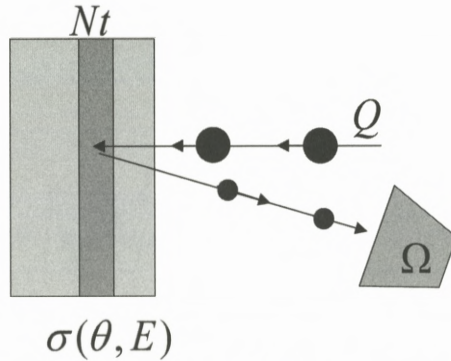
Figure 1. Schematic of a standard RBS set-up indicating the sample-detector configuration and using a solid state detector subtending a solid angle Ω. The measured yield from a thin layer of material of thickness t, volume concentration N may be approximated as $Nt\sigma(\theta, E)\Omega \cdot \Omega$, where $\sigma(\theta, E)$ is the cross-section for scattering to an angle θ and Q represents the number of incident ions.

2. Ion Scattering

The basic physics that governs the interaction of energetic ion beams with solids has its roots in the atomic and nuclear physics of the last century. The central formalisms of Rutherford, Bohr, Lindhard, and others, describing the "ion-solid interaction", provide a valuable quantitative guide to statistically meaningful quantities such as energy loss, ranges, range straggling, channeling effects, sputtering coefficients and damage intensity and profiles. This approach has been an important pillar of the field, leading to a wealth of science and applications. Modern materials science requires atomic scale control and the ability to characterize grown structures on the atomic scale. At this level a reexamination of the ion beam probe is appropriate to either seek enhancements to the technique or to understand the limitations for application at this nanometer level.

Rutherford backscattering has emerged as the most general and used application of ion beam analysis. Indeed both the high level of understanding of the process and its simplicity has combined to underpin this broad application. The process and its description are well-known to the broader community and described in detail in the books by Chu et al. (1978), Feldman and Mayer (1986) and others. The basic scheme is shown in Figure 1. Often RBS is combined with channeling to enhance the surface component of the scattering (Feldman et al., 1982). The apparatus that is employed in RBS also lends itself to a number of other techniques useful in the quantitative analysis of solids. These include particle induced x-ray emission (PIXE), elastic recoil detection analysis (ERDA),
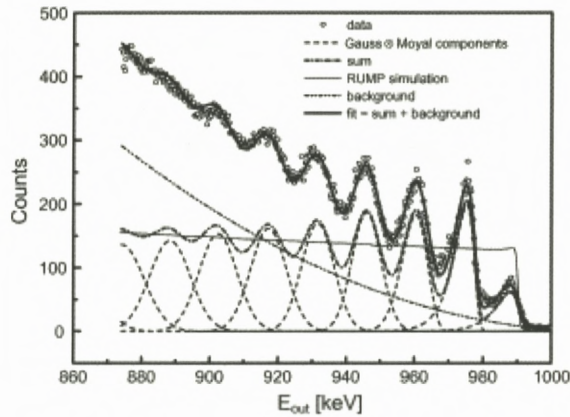
Figure 2. High energy resolution RBS spectrum from a HOPG sample. The first seven carbon layers of the sample are well resolved. (Incident beam: 1 MeV N^+ ions, analyzed ions: N^{2+}, scattering angle: $7°$, angles of incidence and exit: $3.5°$ each.) from Srivastava et al. (2004).

forward recoil scattering (FRS), and nuclear reaction analysis (NRA). Each has their own specific applications. However the straightforward discussion of RBS provides simplicity, while the discussion of limitations may also apply to these other techniques. We first review, with literature examples, the current state of the art of RBS.

2.1. DEPTH RESOLUTION

Depth resolution has been optimized over recent times through the use of new geometries, grazing angle techniques and the use of high resolution spectrometers. The latest probes can achieve monolayer resolution at the surface of a single crystal (Vrijmoeth et al., 1991; Kimura and Mannami, 1996; Srivastava et al., 2004). A famous example, shown in Figure 2, reveals the monolayer-by-monolayer depth resolution that is achievable (Srivastava et al., 2004).

Such depth resolution is satisfactory for the investigation of clean surfaces, a relevant two-dimensional nanostructure. Ion scattering has been an important tool in understanding surface structures, surface adsorption/desorption kinetics, and ultra-thin (of order a few monolayers) film structures.

Nanostructured materials often comprise buried interfaces. The region in the immediate vicinity of the interface, usually less than 100 nm below the surface, is the critical element of these structures. In such cases the exquisite depth resolution afforded by ion scattering probes is dominated by energy straggling. Indeed finite and insufficient depth resolution is a characteristic of almost all material

probes, including electron spectroscopys such as Auger analysis in combination with sputtering where the depth resolution may be defined by sputter induced ion beam mixing; photoelectron spectroscopy, where the depth resolution is defined by the extinction length; and secondary ion mass spectroscopy (SIMS) where the depth resolution may be determined by ion beam mixing. In the ion scattering case the resolution broadening mechanism, straggling, is relatively well understood in terms of the statistical aspects of the energy loss process. Nevertheless for either experimental and/or theoretical reasons the unfolding of the straggling contribution to depth resolution has not yet been established.

2.2. THIN FILM STOICHIOMETRY

As mentioned above the formation of nanostructures often begins with the growth or deposition of a thin film on a substrate. For semiconductor structures the dielectric plays the role of a surface passivator, with the goal of eliminating surface states. In such applications the overlayer dielectric must be of high quality, stoichiometrically ideal and able to withstand high voltages to avoid breakdown.

Ion scattering is an ideal tool for the determination of stoichiometry. Some of the most precise work in this type of problem is reported in the InGaAs system, where the authors report a stoichiometry determination to better than 1% (Jeynes et al., 1997). The limitation of improved stoichiometry determination is primarily the statistical accuracy of an experiment and the knowledge of the scattering cross-section to considerably better than 1%.

2.3. ULTIMATE SENSITIVITY

In many applications it is critical to explore impurity levels at very low concentrations. For semiconductor/dielectric problems this often means at the impurity level that can affect the electronic properties of the material, as small as $10^{10}/cm^2$.

The ultimate sensitivity of the ion beam probe is discussed by Feldman and Mayer (1986). Basically the technique is limited by the ion beam sputtering process. Obviously one requires that the probing beam not remove (sputter) the impurity before the completion of the analysis. Such a formulation can be quantitatively established using accepted formulae for ion scattering and sputtering yields. Questions of the appropriate sputtering coefficient to apply to the ultimate surface problem persist. How do you describe the sputtering coefficient for a small fraction of Au on a silicon substrate?

Ultimate sensitivity in ion scattering has been established by the Sandia group (Banks et al., 1998) using low energy – heavy ion beams, time-of flight detection techniques and optimal geometries. This work shows detection sensitivities of

$\sim 1 \times 10^{10}/cm^2$, an amazing result and certainly in the range where correlation with electrical measurements would be meaningful.

2.4. LATERAL RESOLUTION

Lateral resolution, comparable to electron beam spectroscopy, has long been a goal of the ion beam community. Recent years have seen an explosion of developments in the ability to develop such beams using a variety of focusing tools and elements. Current limits are at the 100 nm level and it seems difficult to achieve smaller spot size. (One caveat – the conventional focused ion beam tool typically produces a $\sim$10 nm 30 KeV Ga beam. This paper concentrates on the higher energy regime but one can expect substantial progress in this area, with higher energy and multiple ion beams). Issues associated with the effects of ion source brightness on nuclear microprobe performance is described in the work of Szymanski and Jamieson (1997). Practical examples of $\sim$500 nm ion beam analysis are given in Dollinger et al. (2006).

A new development in focused ion beams is the use of tapered glass capillary optics (Nebiki et al., 2003). In this procedure glass capillaries are formed with opening apertures of $\sim$1 mm and outlet diameters of sub-microns. A surface channeling effect is involved which results in approximately 1% of the beam forming a suitable analysis beam. Although the beam loss is large, and there is some loss of energy resolution due to side-wall scattering, this may be a most convenient and useful mode of placing ion beam analysis in the sub-micron regime. Clearly such simplified and useful methods of forming focused ion beams will receive considerable attention in the future.

3. Semiconductor-Dielectric Interfaces

In the following we illustrate RBS analysis of a number of semiconductor dielectric interfaces. It should be remembered that each of these studies is a multi-technique investigation involving a substantial number of electronic and structural probes. The following discussion focuses only on the ion scattering part to reveal the strengths and limitations of this aspect of particle-solid interactions.

3.1. THE Si/SiO$_2$ INTERFACE

To a large extent the silicon revolution is based on the wonderful properties of the silicon/silicon dioxide interface (Queisser, 1998). The importance of this structure has been documented and cited in many articles and books on the history of technology. Clearly it is the most important materials interface in current process

technologies. Briefly, oxidation of pure silicon results in a large band-gap, uniform, dielectric layer of amorphous SiO_2, with the proper band-offsets to allow both p and n channel devices to be fabricated. Most importantly, modern growth and annealing techniques result in interface defect levels that are sufficiently small so that carrier transport is close to theoretical limits. These excellent qualities have served the community well and been preserved as the basic metal-oxide-semiconductor field effect transistor (MOSFET) device has scaled down over the last five decades.

The success of the MOSFET hinged on a most important and fundamental element of solids, namely the limitations imposed by surface states. Even ideal surfaces can possess electronic states that represent sufficient charge to make the MOSFET inoperable. Hans Quiesser, in his exciting book, *Conquest of the Microchip*, notes: "what finally saved the day was that an incredibly stable oxide of silicon can be wrapped around the crystal to protect it" (Queisser, 1998). Another historical account, *The History of Engineering & Science in the Bell System* (Millman, 1983), states "surface state problems were resolved by an unexpected discovery .... Kahng and Atalla found that silicon and clean, thermally grown SiO_2 interfaces contain sufficiently small surface states to realize a true field effect transistor in silicon". Frosch and Derick (1957) first reported the beneficial properties of the SiO_2/Si materials system.

Research in the last twenty years has exploited almost every conceivable surface/thin film probe to establish the underlying physical nature of this critical solid-state interface (Feldman et al., 1998). Of particular interest has been the nature of the starting silicon surface, the kinetics of the oxidation process, the structure and solid-state chemistry of the silicon-silicon dioxide interface and the relationship of the structure to the electronic properties.

Nevertheless outstanding scientific issues remain at the very forefront, limiting the further evolution of silicon science and technology. Indeed these issues have become even more prominent. For as the device has scaled down, with the corresponding reduction of silicon dioxide thickness from microns to nanometers, the silicon/silicon dioxide interface becomes more prominent and more limiting. We are close to fundamental limits where the need for understanding and atomic control becomes ever more critical.

Ion-scattering experiments
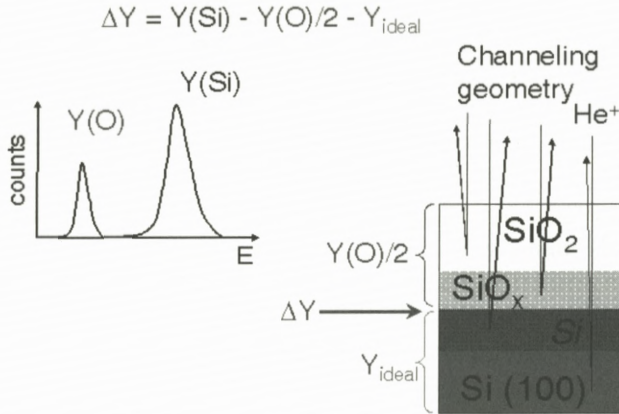
$$\Delta Y = Y(Si) - Y(O)/2 - Y_{ideal}$$

Figure 3. Schematic of the ion scattering/channeling configuration with the beam oriented parallel to the major $\langle 100 \rangle$ channeling direction for a Si/SiO$_2$ structure. The spectrum schematically indicates the scattering from the oxygen in the oxide and the silicon contributions from the SiO$_2$, the SiO$_x$ and the Si surface peak. The "excess yield", ΔY, is indicated as the silicon yield over and above that expected from an ideal, stoichiometric oxide and Y_{ideal}, the contribution from the ideal surface peak.

It is generally agreed that there is a transition region (of altered structure and/or stoichiometry) between crystalline silicon and SiO$_2$. Ion scattering experiments on this interface have contributed to the sophisticated characterization required for the determination of the structure (Bongiorno et al., 2003). Measurements are usually done in a channeling geometry as shown schematically in Figure 3. Because of the channeling condition the ion scattering spectrum is dominated by silicon and oxygen in the amorphous oxide and the Si surface peak, as shown in Figures 3 and 4.

In a channeling direction the ion beam encounters at least the first monolayer of a clean surface with a full scattering intensity. Scattering from deeper layers is suppressed due to the channeling (shadowing) effect. In practice the "surface peak" encompasses scattering yields from the first few monolayers of the solid due to thermal vibrations, which cause the first few sub-surface layer atoms to extend beyond the shadow established by the first atom in the string. The total yield of surface scattering for an ideal crystal can be estimated through a variety of numerical simulations (Feldman et al., 1982). Figure 5b shows the good agreement between the measured and calculated surface scattering intensity for the Si(100)-H-(1×1) surface, a surface structure that is established to have a near "bulk-like"
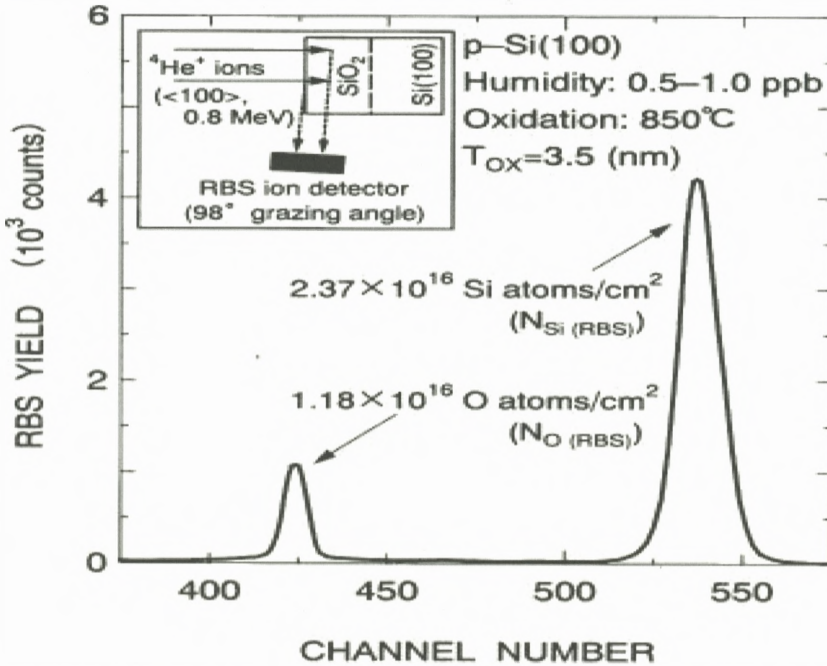
Figure 4. Rutherford backscattering spectrometry (RBS) spectrum for the 3.5 nm-thick silicon oxide film grown on a *p*-type Si(100) substrate at 850°C with 0.5–1.0 ppb humidity. This was obtained in the channeling grazing-exit-angle geometry using 0.8 MeV ^{4}He$^+$ incident ions along a Si $\langle 100 \rangle$ -axial-aligned channeling direction and an ion detector arranged at a grazing-exit angle of 95° relative to the incident ion beam (Yamada, 2001).

surface termination. The good agreement between experiment and calculation for the "bulk-like" surface establishes the validity of the technique and the value of the intrinsic surface contribution to the total silicon scattering intensity (Stensgaard et al., 1981).

The essential results of the measurements indicates an excess of Si scattering over that expected from an ideal structure for the Si/SiO$_2$ material (Jackman et al., 1980). This excess is attributed to the distortion of the first few monolayers of silicon at the amorphous oxide/crystal interface. This "excess" has been compared to theory (Bongiorno et al., 2003) to provide a total description of the interface structure and distortions (Figure 5). The significance of these few monolayers of distortion may be understood when it is realized that the electronic wave function of the conduction electrons is confined to ~10 monolayers near the interface and the crystal distortion can seriously affect the electron probability density and the (inversion layer) electron mobility. This latter quantity ultimately determines
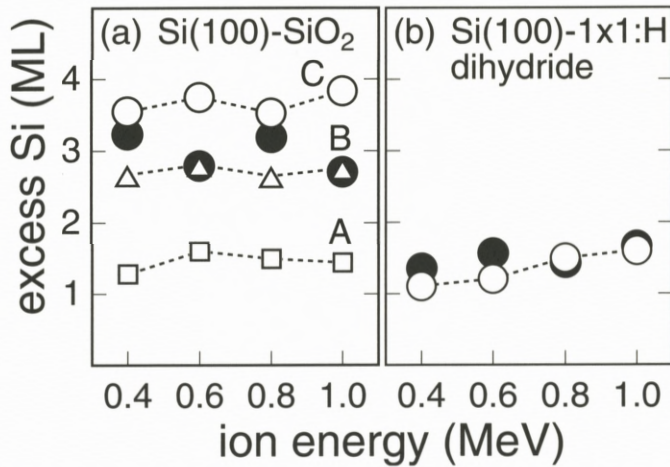
Figure 5. Measured (full circles) and calculated excess Si yields *versus* ion energy for (a) the Si(100)-SiO$_2$ interface and (b) the Si(100) 1×1:H surface. The agreement for the hydrogen termi-nated surface demonstrates the high level of understanding of the intrinsic surface peak. In (a) the calculated values are obtained for different models of the interface structures; the contribution from partially oxidized silicon is shown by a shaded band. The models are most completely explained in Bongiorno et al. (2003), but may be briefly described as (A) near ideal termination with no distruption; (B) in-plane dimers and (C) a mixture of dimers and nonstoichiometric oxide.

the speed of the device. Other authors have also measured this Si distortion and considered its extent as a function of oxidation parameters (Stedile et al., 1996; Yamada, 2001, 2002).

3.2. "ALTERNATE" DIELECTRICS-NECESSITY OF HIGH K MATERIALS

One of the fundamental limits of ultrathin oxide/oxynitride films is direct tunnel-ing (current) which grows exponentially with decreasing film thickness (Feldman et al., 1998). For sub 2 nm films, the tunneling current becomes large, which requires a significant (and unacceptable) power dissipation in logic devices, es-pecially for portable applications. To overcome the direct tunneling problem, the "physical" thickness of the dielectric should be kept large, much thicker than the direct tunneling limit ~2.0 nm. On the other hand, ULSI scaling is driving a re-duction in thickness (increasing capacitance) for next generation of fast switching devices. One way to ameliorate these conflicting needs is to replace conventional SiO$_2$ by a material with a higher dielectric constant, preferably a much higher one. This would allow a dielectric with a thicker "physical" thickness, but the "equiv-alent" capacitance (with respect to pure SiO$_2$) and the direct tunneling current would be much reduced.

Several high K materials are now being explored as a gate dielectric. Recent examples include ZrO_2, HfO_2, hafnium silicates, scandium oxide and others. The material of choice must have a set of important properties including: (i) a high dielectric constant (preferably > 25), (ii) high thermal stability (especially with respect to Si); (iii) perfect stoichiometry (which presumably minimizes intrinsic defects and traps in the film), (iv) a low concentration of interface states and stability of the interface during thermal treatments and external radiation; (v) resistance to dopant diffusion, (vi) low leakage currents; (vii) large band gap (>4 eV) and an appropriate barrier offset with respect to silicon; (viii) a low thermal budget, defect free processing; and (ix) manufacturability and integration with silicon technology. Ideally, this material should have properties as good as SiO_2 on Si, but with a much higher dielectric constant. This is a "tall order" and there is no clear favorite at the moment. The search for the alternate dielectric is an intense on-going activity in the semiconductor community.

Furthermore, a very thin buffer layer of silicon oxide, oxynitride or nitride may still be required between the silicon substrate and the high K dielectric in order to minimize interface states and to act as a diffusion barrier between the layers. In this case, the equivalent thickness of the stacked dielectric will have contributions from both the thickness of the buffer layer and the equivalent thickness of the high K layer. To keep the overall equivalent thickness less than ~ 1.0 nm, the buffer layer should consist of not more than 1–2 atomic layers. Needless to say, this mono/double layer should be nearly perfect and the new interface between the buffer layer and the high K material should be as high quality as the SiO_2/Si interface. This fact motivates and justifies the continuing, atomic-scale studies of ultrathin silicon oxides, oxynitrides and nitrides, in conjunction with the exploration of the optimum alternate dielectric.

Ion scattering analysis plays a significant role in the search for the "alternate dielectric" (Gustafsson et al., 2001). Figure 6 shows an important contribution of ion scattering for the case of a ZrO_2 layer. With the clever use of isotopes and making use of the mass selectivity and depth resolution of ion scattering the authors show that oxidation (in ^{18}O) of a SiO_2/ZrO_2 stack results in oxygen exchange within the ZrO_2 and additional oxidation of the underlying silicon increasing the underlying SiO_2 layer. Such results are critical to questions of reliability and processing of these new structures.

3.3. SiC/SiO$_2$

Si-based metal-oxide-semiconductor field-effect transistors are at the heart of microelectronics. However, for many applications, such as systems operating at high power, high temperature, and high frequency, it is very desirable to have
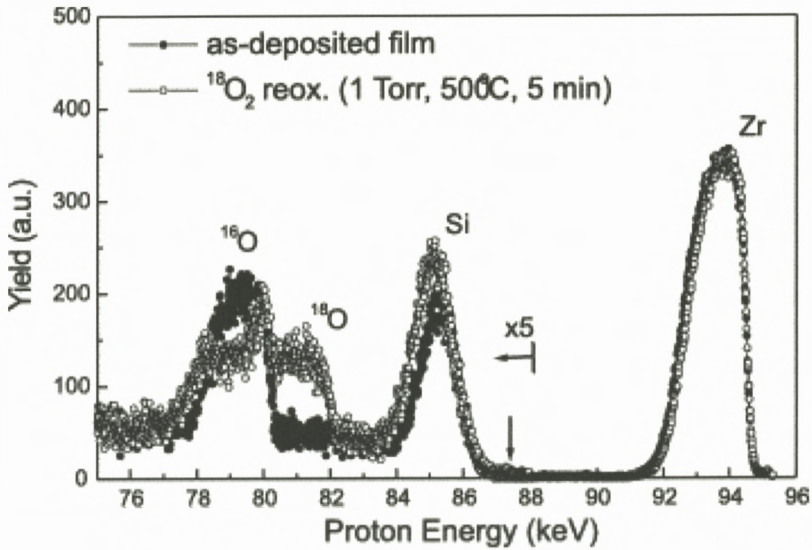
Figure 6. Medium Energy Ion Scattering (MEIS) proton spectrum from the as-deposited ZrO_2 film on Si(100), and a film subsequently re-oxidized in $^{18}O_2$ (1 Torr, 500°C, 5 min). Signals from ^{16}O, ^{18}O, Si and Zr are clearly resolved. The arrow at 87.3 keV indicates the energy where surface Si would be detected. The data clearly show the growth of SiO_2 at the interface between the ZrO_2 film and Si substrate (as seen by shifts of the O and Si signals to lower energy), and a dramatic oxygen exchange within the film (Gustafsson et al., 2001).

MOSFETs based on a wide-band-gap semiconductor. High temperature at high power operation has become increasingly important as society considers energy efficient systems.

Several wide-band-gap semiconductors have been investigated extensively, but all are limited by the lack of a suitable dielectric. The problem is generic as Si-SiO_2 is the only semiconductor-dielectric combination that yields functional MOSFETs. No other semiconductor has a native oxide that meets the crucial requirements of low densities of interface traps that control channel mobility. Deposited non-native oxides have not proven adequate either. From this perspective, SiC is a unique semiconductor because it is the only other material, besides Si, whose native oxide is the well understood SiO_2. 4H-SiC also has high thermal conductivity, high breakdown field strength, reasonable mobility and mobility anisotropy and high saturated electron drift velocity, all of which make it a prime candidate for high-power, high-temperature, and high-frequency devices. Obviously the critical role of the dielectric requires that the material, its stoichiometry and its electrical properties be well characterized and understood. The stoichiom-
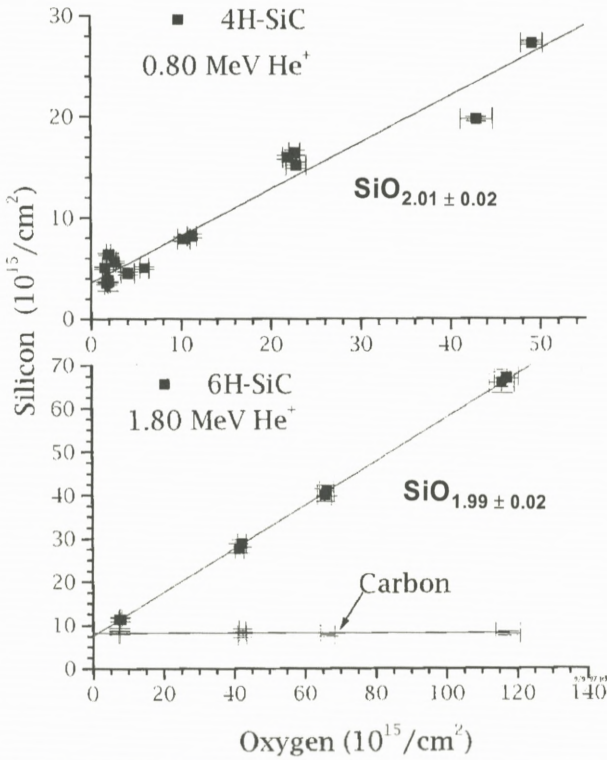
Figure 7. Determination of the Si to oxygen ratio as a function of thickness for SiO_2 grown layers on SiC. The values of the slope of the line indicate that the oxide is stoichiomentric SiO_2. The y-axis intercept is a measure of the intrinsic Si surface intensity. Note that the carbon content, which arises from the crystalline carbon surface peak, is constant with growth indicating no carbon incorporation (at the level of $10^{15}/cm^2$) in the oxide.

etry determination is an ideal problem for ion beam analysis. Figure 7, shows the results of ion scattering studies, in a channeling direction, to determine the composition of the grown oxide on 4H-SiC. Clearly the material is stoichimeteric SiO_2, within the error of the determination. Furthermore, there is essentially no carbon within the film. The baseline of the carbon content arises from the carbon surface peak and is constant with increasing oxide thickness. Such measurements, as a function of processing conditions and in concert with other experimental studies, demonstrate that the oxide is essentially pure SiO_2, similar in all ways to the high quality oxide on Si. The successful growth of this oxide followed by specialized processing has opened up the possibility for a new high power, energy efficient SiC technology (Song et al., 2004).

3.4. CdSe QUANTUM DOTS

Nanostructures, particularly "quantum dots", with their very large surface to volume ratio and their non-planar geometry, present an important challenge to surface scientists. New issues arise as to surface characterization, quantification, and interface formation and surface passivation.

A nanocrystal is essentially a three-dimensional quantum square well. By precisely controlling a nanocrystal's size and surface, its properties can be engineered. CdSe nanocrystals vary in size from ~2–11 nm and contain a few hundred to ten thousand atoms. Through quantum confinement of the photo-created electron hole pair the optical properties of the nanocrystal can be tuned by size. For example, a 2.2 nm nanocrystal will have 88% of its atoms on the surface and absorb light at 420 nm while a 8.5 nm nanocrystals consists of 20% surface atoms and absorbs light at 650 nm. Nanocrystals are usually chemically synthesized in an organic surfactant that passivates the surface. The choice of surfactant can control the growth of the nanocrystal and its size and shape. The surfactant/nanocrystal organic/inorganic interface also controls the ultra-fast carrier dynamics in the nanocrystal and the fluorescence quantum yield. Alternatively the surface of the CdSe nanocrystal can be passivated with a second inorganic material, such as CdS, ZnS, or ZnSe to create a core-shell nanocrystal. When wrapped in a wider band gap material the electron-hole pair is further confined and surface states dangling bonds are minimized. If the interface between the two inorganics is perfect nearly unity quantum yield materials result. Here again characterization of the interface is crucial in order to engineer a quantum dot with desired properties (McBride et al., 2006).

Given their large surface to volume ratio and their non-planar geometry, nanocrystals present an important challenge to surface scientists. Recent investigations use Rutherford backscattering spectroscopy (RBS) and atomic number-contrast scanning transmission electron microscopy (Z-STEM) to determine composition and size (McBride et al., 2006). When combined these techniques give information on nanocrystal composition, surface composition, surface ligand coverage, and nanocrystal structure, including the interior, interfaces, and surfaces of the quantum dot.

Figure 8 shows an example of the insights to be gained by the accuracy afforded in a stoichiometry measurement via RBS. Here the quantity of interest is the stoichiometry as accurately determined via the Cd/Se ratio. Systematic studies as a function of size and crystal growth procedures revealed that nanocrystals grown in TOPO (trioctyphosphine oxide) showed excess Cd. The systematic
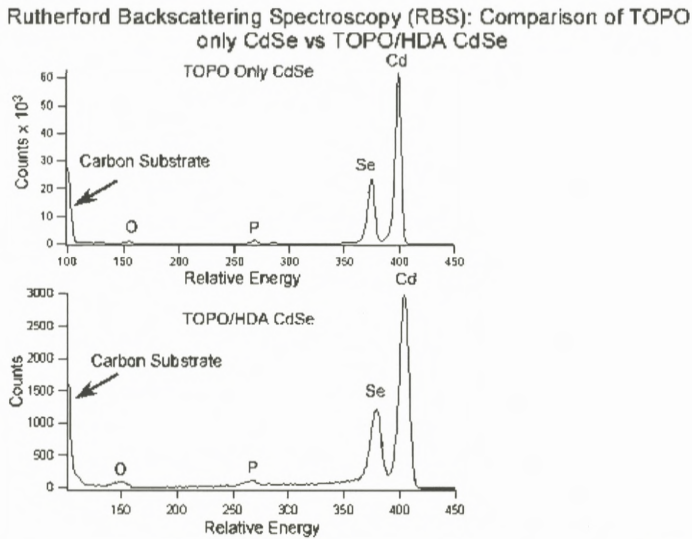
Figure 8. RBS spectrum comparison of CdSe nanocrystals grown in TOPO and HAD. The ideal stoichiometry, 1:1, is achieved in the HAD grown material leading to more uniform size distributions and more efficient optical properties (McBride et al., 2006).

series of measurements indicate that the excess was a surface component, easily envisioned when it is recognized that the surface contains ~50% of all the atoms in the structure. Growth in hexadecylamine (HAD) results in a stoichiometric nanocrystal with superior surface properties, compared to growth in TOPO. These core structures may then be encapsulated in a wide-band gap semiconductor to provide surface passivation and reduce surface recombination.

The RBS analysis reveals intriguing insight in the structure of these TOPO only nanocrystals. The excess Cd is due to the stabilization of Cd dangling bonds by the passivating TOPO. An outcome of this analysis was the successful capping of the stoichiometric nanocrystals with a wide band gap semiconductor, ZnCdS. The wide band gap material plays the same role in these nanocrystals as SiO_2 on Si-namely it passivates surface states. The final structure had exceedingly high quantum yields of >80%, indicative of a well passivated surface.

4. Conclusions and Questions

These examples illuminate the strengths, weaknesses and physical limitations of ion scattering spectroscopy. It is important to distinguish between limitations that

arise because of well-understood physics and limitations that might be overcome with new experimental and computational approaches.

A complete discussion of the limitations to depth resolution in ion scattering experiments has recently been presented by Schulte et al., focusing on the shape of the surface peak in "clean surface" experiments (Schulte et al., 2001). Good agreement between experiment and theory depends on the understanding of the impact parameter dependent stopping power, understanding the thermal vibrations of surface atoms, and the possibility of specific inelastic losses. All of these quantities require further testing and more precise comparisons between experiment and theory. A fascinating aspect of this question is the possible effects of modified energy loss and energy loss straggling in these lower dimensional structures consisting of a two-dimensional electron gas (Borisov et al., 2006).

Buried interfaces provide an additional set of issues for the ion scattering community. Undoubtedly new methods to deconvolute straggling contributions could be a substantial benefit in analysis. This is a formidable task both experimentally and theoretically. Nevertheless success in this venture will represent a substantial benefit and applicability to the technique. It is clear that all of the buried structures described above would benefit from a sophisticated deconvolution of the straggling contribution to the resolution broadening.

On the experimental side there needs to be considerable efforts at higher resolution and more efficient detectors. Efficiency here might mean the ability for three dimensional analysis in the channeling-blocking configuration, to minimize ion beam damage. The convenience of the solid state detector also needs to be recognized. The great advances that have occurred in semiconductor heterostructures suggest that new solid state detectors might be conceived with better energy resolution.

Many contributions to nanoscience will depend on the successful utilization of focused ion beams. It is important to explore new and convenient ways of forming such beams, with optimal geometries to reduce probing beam damage effects. The glass capillary approach mentioned above is such an example (Nebiki et al., 2003).

Finally, as noted above, thin film stoichiometry is a great strength of the RBS technique. In the limit of high statistical accuracy the stoichiometric determination will be limited by absolute knowledge of the scattering cross-sections, indicating the need for more precise measurements of these fundamental quantities, particularly for low Z elements.

All of the examples cited above could yield more detailed and specific information with the potential advances cited above.

Acknowledgements

It is a pleasure to acknowledge colleagues with whom I have collaborated concerning the issues discussed in this manuscript: S.J. Rosenthal, J. McBride, S. Dhar, Y. Song, S. Dixit, J. Williams, A. Bongiorno and A. Pasquarello.

References

Banks J.C., Doyle B.L., Knapp J.A., Werho D., Gregory R.B., Anthony M., Hurd T.Q. and Diebold A.C. (1998): Using Heavy Ion Backscattering Spectrometry (HIBS) to solve integrated circuit manufacturing problems. Nucl Instrum Meth Phys Res B **137**, 1223–1228

Bongiorno A., Pasquarello A., Hybertson M.S. and Feldman L.C. (2003): Transition structure at the Si(100)-SiO_2 interface. Phys Rev Lett **90**, 186101

Borisov A.G., Juaristi J.I., Muino R.D., Sanchez-Portal D. and Echenique P.M. (2006): Quantum size effects in the energy loss of charged particles interacting with confined two-dimsional electron gas. Phys Rev A **73, no. 1**, 012901

Chu W.K., Mayer J.W. and Nicolet M.A. (1978): Backscattering Spectrometry. Academic Press, New York

Dollinger G., Bergmaier A., Hauptner A., Dietzel S., Drexler G.A., Greubel C., Hable V., Relchart P., Krucken R., Cremer T. and Friedl A.A. (2006): Hydrogen microscopy and analysis of DNA repair using focused high energy ion beans. Nucl Instr Meth Phys **249**, 270–277

Feldman L.C. and Mayer J.W. (1986): Fundamentals of Surface and Thin Film Analysis. North Holland-Elsevier, New York [Translated into Japanese, Kaibundo Publishing (1988); translated into Russian, MIR Publishing (1989)]

Feldman L.C., Mayer J.W. and Picraux T.A. (1982): Materials Analysis by Ion Channeling: Submicron Crystallography. Academic Press, New York

Feldman L.C., Gusev E.P. and Garfunkel E. (1998): Ultrathin dielectrics in Si microelectronics – An overview. In: Garfunkel E., Gusev E.P. and Yavul A. (Eds), Fundamental Aspects of Ultrathin Dielectrics on Si-Based Devices. Kluwer Academic Publishers, Dordrecht

Frosch C.J. and Derick L. (1957): Surface protection and selective masking during diffusion in silicon. Proc Electrochem Soc **547**

Gustafsson T., Lu H.C., Busch B.W., Schulte W.H. and Garfunkel E. (2001): High-resolution depth profiling of ultrathin gate oxides using medium-energy ion scattering. Nucl Instrum Meth Phys Res B **183**, 146–153

Jackman T.E., MacDonald J.R., Feldman L.C., Silverman P.J. and Stensgaard I. (1980): (100) and (110) Si-SiO_2 interface studies by MeV ion backscattering. Surf Sci **100**, 35–41

Jeynes C., Jafri Z.H., Webb R.P., Kimber A.C. and Ashwin M.J. (1997): Accurate RBS measurements of the indium content of InGaAs thin films. Surf Sci Interface Anal **25**, 254

Kimura K., and Mannami M. (1996): RBS single monolayer resolution. Nucl Instrum Meth Phys Res B **113**, 270

McBride J., Treadway J., Feldman L.C., Pennycook S.J. and Rosenthal S.J. (2006): Structeral basis for near unity quantum yield core/shell nanostructures. NanoLetters **6**, 1496

Millman, S. (Ed.) (1983): A History of Engineering and Science in the Bell System. AT&T Bell Laboratories, New York

Nebiki T., Yamamoto T., Narusawa T., Breese M.B.H., Teo E.J. and Watt F. (2003): Focusing of MeV ion beams by means of tapered glass capillary optics. J Vac Sci Technol A **21**, 1671–1674

Queisser H. (1998): The Conquest of the Microchip. Harvard University Press, Cambridge, MA

Schulte W.H., Busch B.W., Garfukel E., Gustafsson T., Schwietz G. and Grande P.L. (2001): Limitations to depth resolution in ion scattering experiments. Nucl Instr Meth B **183**, 16

Song Y., Dhar S., Feldman L.C., Chung G. and Williams J.R. (2004): Modified deal grove model for the thermal oxidation of silicon carbide. J Appl Phys **95**, 4953–4957

Srivastava S.K., Plachke D., Szokefalvi-Nagy A., Major J. and Carstanjen H.D. (2004): Counting individual atom layers in graphite – High-resolution RBS experiments on highly oriented pyrolytic graphite. Nucl Instrum Meth Phys Res B **219/220**, 364

Stedile F.C., Baumvol I.J.R., Oppenheim I.F., Trimaille I., Ganem J.J. and Rigo S. (1996): Thickness of the SiO_2/Si interface and composition of silicon oxide thin films: Effect of wafer cleaning procedures. Nucl Instrum Meth Phys Res B **118**, 493–498

Stensgaard I., Feldman L.C. and Silverman P.J. (1981): Evidence of multilayer distortions in the reconstructed Si(001) surface. Surf Sci **102**, 1–6

Szymanski R. and Jamieson D.N. (1997): Ion source brightness and nuclear microprobe applications. Nucl Instrum Meth Phys Res B **130**, 80–85

Taylor J., Kippeny T., Bennett J.A., Huang M., Feldman L.C. and Rosenthal S.J. (1999): Proceedings of the Materials Research Society, Microcrystalline and Nanocrystalline Semiconductors, Vol 536, p 413.

Vrijmoeth J., Zagwijn P.M., Frenken J.W.M. and Vanderveen J.F. (1991): Monolayer resolution in medium-energy ion-scattering experiments on the $NiSi_2(111)$ surface. Phys Rev Lett **67**, 1134–137

Yamada H. (2001): Microscopic composition difference related to oxidizing humidity near the ultrathin silicon oxide-Si(100) interface. J Vac Sci A **19**, 627

Yamada H. (2002): Changes in the density of ultrathin silicon oxide films related to excess Si atoms near the oxide-Si(100) interface. J Appl Phys **91**, 1108